



# Microwave Radiometric Mapping of Broken Cumulus Cloud Fields from Space: Numerical Simulations

Yaroslav Koptcov<sup>1</sup>, Yaroslav Ilyushin<sup>1,2</sup>(✉), Boris Kutuza<sup>2</sup>,  
and Dobroslav Egorov<sup>2</sup>

<sup>1</sup> Physical Faculty, Moscow State University, Moscow, Russia  
koptcov.iv17@physics.msu.ru, ilyushin@phys.msu.ru

<sup>2</sup> Kotel'nikov Institute of Radio Engineering and Electronics,  
Russian Academy of Sciences, Moscow, Russia  
kutuza@cplire.ru

**Abstract.** Monitoring the atmosphere characteristics is an important task in remote sensing of the environment. In this paper, the question is raised about taking into account the influence of clouds on the characteristics of thermal radiation. The aim is to analyze the applicability of models for cloud correction during microwave radio sounding of thermal radiation. The result of the work is to determine the parameters that best correspond to the cloud fields of the Earth's atmosphere.

For the applicability of the calculated values to account for the structure of clouds in the atmosphere, it is necessary to generate model cloud fields comparable in size to real cloud fields in the Earth's troposphere. This results in significant computational costs required for their modeling and analysis.

Numerical modeling of the statistical properties of thermal radio emission of separated cloudiness field models implies the need to perform calculations with an ensemble of simulated random fields of a sufficiently large size, and the use of projections with good resolution, therefore, the optimal use for computing high-performance computers.

As a result, the developed algorithms and computer models of cloud fields significantly form a practical basis for further studies of radiation processes in the cloud atmosphere. Two-dimensional (2D) distributions of the brightness temperature of the outgoing thermal radiation of the separated cloudiness fields were calculated. For simplified statistical models of separated cloudiness fields, numerical estimates of the radio brightness temperatures of microwave radiation of the cloud layer are obtained depending on the model statistical parameters.

**Keywords:** Plank model · Cumulus clouds · Microwave radiometric sensing

## 1 Introduction

Monitoring of atmospheric characteristics is an important task in remote sensing of the environment. In this paper, the question is raised about taking into

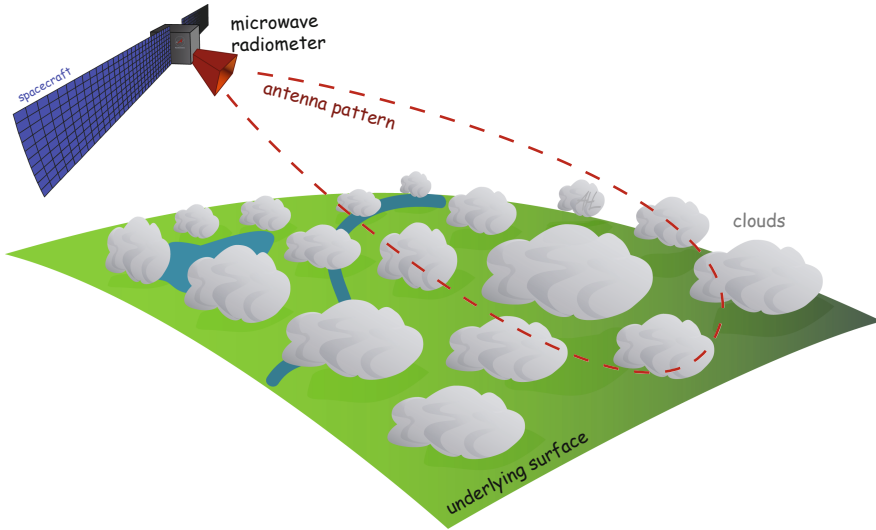


**Fig. 1.** General sketch of the experimental radiometry of cloud fields.

account the influence of clouds on the characteristics of thermal radiation. Atmospheric sounding by the method of receiving atmospheric thermal radiation is the development of ground-based studies of atmospheric thermal radiation. One of the methods of such research is microwave radiometric sounding from artificial Earth satellites. Passive microwave radiometry [1–5] has long been used as a remote sensing approach in geophysics [7,8], meteorology [9] and astronomy [6,10,11]. Observations of the thermal radiation of the atmosphere-ocean surface system [13–15] allow us to obtain information about the state of cloud fields in the atmosphere and quantify many meteorological parameters, for example, the mass of water vapor [18], water reserve [17] and the effective temperature of clouds [16]. The disadvantage of a significant part of most previous studies is the use of a homogeneous plane-layered model of the cloud layer, ignoring its heterogeneous structure [20].

Clouds in the troposphere are involved in the scattering and reflection of sunlight and thermal radiation of the atmosphere. For this reason, cloud cover makes a significant contribution to the radiation and energy balance of the atmosphere, which plays a key role in climatic processes on the planet. To understand this role, it is necessary to study the radiation properties of cloud cover. Cloud fields are characterized by a random structure, so their properties are random and can be studied by statistical methods. One of the possible approaches is a direct numerical evaluation of the properties of the cloud fields of interest based on their specific implementations, followed by averaging. This approach is also used in this study.

The aim of this work is to numerically simulate the statistical properties of the thermal radio emission of Plank fields of broken clouds in the microwave range

and to study systematic errors of meteorological parameters of the atmosphere associated with the random nature of real broken cloud fields. For this purpose, direct numerical modeling of cloud fields is carried out in the work and the characteristics determining the radio brightness temperatures of broken clouds at various frequencies of the microwave wavelength range are calculated. The calculated characteristics are directly compared with the results obtained in the works of other authors in the study of real fields of broken clouds.

## 2 Size Distributions and Geometry of Broken Cloud Fields

In the article [12] it is shown that when calculating the characteristics of radiation fields in the microwave range, the assumption of the cylindrical shape of clouds is acceptable.

### 2.1 The Plank Model

Plank [22] proposed the following distribution:

$$n(D) = Ke^{-\alpha D}, \quad 0 \leq D \leq D_m \quad (1)$$

where  $D$  is the diameter of the cloud,  $D_m$  is the maximum possible diameter of the cloud in the field,  $K$  is a normalization constant,  $\alpha$  is a constant parameter depending on local conditions [22].

The cumulative distribution of the number of clouds by size is, respectively, equal to:

$$N(D) = \frac{1 - e^{-\alpha D}}{1 - e^{-\alpha D_m}} \quad (2)$$

Average diameter of clouds:

$$\langle D \rangle = D_m \left( \frac{1}{\alpha D_m} - \frac{1}{e^{\alpha D_m} - 1} \right) \quad (3)$$

### 2.2 Alternative Model

Distribution proposed in [19] based on aircraft measurements over Ukraine:

$$n(D) = KD \cdot \left( 1 - \frac{D}{D_m} \right)^{p_0}, \quad 0 \leq D \leq D_m \quad (4)$$

where  $D$  is the diameter of the cloud,  $D_m$  is the maximum possible diameter of the cloud in the field,  $K$  is a normalization constant,  $p_0$  is a constant parameter depending on local conditions [19].

The cumulative distribution of the number of clouds by size is, respectively, writes as follows:

$$N(D) = 1 - \left( (1 + p_0) \frac{D}{D_m} + 1 \right) \left( 1 - \frac{D}{D_m} \right)^{p_0+1} \tag{5}$$

Average diameter of clouds, respectively, is

$$\langle D \rangle = \frac{2D_m}{3 + p_0} \tag{6}$$

### 2.3 The Cloud Height Distribution

Following the work of [22], the power of the cloud and its diameter can be linked unambiguously by the ratio:

$$H = \eta D \left( \frac{D}{D_m} \right)^\beta \tag{7}$$

where  $\eta$  and  $\beta$  are the adjustable model parameters.

Since the height of the cloud is unambiguously related to its diameter by the formula (7), the cloud height in the cloud field is also a random variable with the corresponding statistical distribution. Since in a given model the height of a cloud is uniquely related to its diameter, the probability density of the height distribution is

$$p(H) = \frac{1}{N(D_m)} n(D) \frac{dD(H)}{dH} \tag{8}$$

where  $N(D_m)$  is the total number of clouds in the field. So a certain density of the distribution of random heights of clouds (8) obviously satisfies the condition of normalization by one

$$\int_0^{D_m} p(H) dH = 1 \tag{9}$$

In frequency, for the Plank model of broken clouds (1) probability density of the cloud height distribution  $p(H)$  is equal to

$$P(H) = \frac{(D_m/(\alpha\eta H))^{\beta/(\beta+1)}}{(1 - e^{-\alpha D_m}) (\beta + 1)} \exp \left( -(D_m/\alpha\eta)^{\beta/(\beta+1)} H^{1/(\beta+1)} \right) \tag{10}$$

For the non-Plank model (4) the density function of the height probability distribution is

$$P(H) = \frac{(p_0 + 1)(p_0 + 2)\eta^{2\beta/(\beta+1)}}{H^{(1-\beta)/(\beta+1)} D_m^{2/(1+\beta)} (\beta + 1)} \left( 1 - \left( \frac{H}{\eta^\beta D_m} \right)^{1/(\beta+1)} \right)^{p_0} \tag{11}$$

It is obvious that the essential parameters of both cloud abundance distributions by diameter (1) and (4) and the corresponding cloud height distributions (10) and (11), the dependence on which is not reduced to a simple linear scaling of the values and arguments of the distribution functions, are in and, respectively,  $\alpha$  and  $p_0$ . Otherwise, these distributions can be reduced to dimensionless normalized parameters  $D/D_m$  and  $H/\eta D_m$ . In practice, this means that in further research, the values of the parameters  $\eta$  and  $D_m$  can be assumed to be equal to one without limitation of generality. Then, in particular, for  $\beta = 0, \eta = 1, D_m = 1$  for the non-Plank cloud model (11) we get

$$p(H) = (1 - H)^{p_0} H (p_0 + 1) (p_0 + 2) \quad (12)$$

This height distribution has a well-defined maximum at  $H = (1 + p_0)^{-1}$ . For  $\beta = 1/2, \eta = 1, D_m = 1$ , respectively, the distribution (11) takes the form

$$p(H) = \frac{2}{3} \left(1 - H^{2/3}\right)^{p_0} \cdot \sqrt[3]{H} (p_0 + 1) (p_0 + 2) \quad (13)$$

with a maximum at

$$H = \frac{1}{\sqrt{8p_0^3 + 12p_0^2 + 6p_0 + 1}} \quad (14)$$

For  $\beta = -1/2, \eta = 1, D_m = 1$ , respectively, the distribution (11) takes the form

$$p(H) = 2H^3 (1 - H^2)^{p_0} (p_0 + 1) (p_0 + 2) \quad (15)$$

with a maximum at

$$H = \frac{\sqrt{3}}{\sqrt{2p_0 + 3}} \quad (16)$$

Probability density distributions (12), (13) and (15) for different values of the parameter  $p_0$  are shown in Figs. 2, 3 and 4, respectively. Thus, these random models of broken clouds can be identified with one of the types of cumulus clouds Cumulus [30] by matching the height of the clouds (according to the maximum probability of distribution or average values) by selecting appropriate combinations of model parameters.

We developed a simple numerical procedure which generates the set of randomly distributed diameters of clouds and then places it randomly over the given rectangular area. The calculation was carried out in the C++ programming language using Intel C++ compiler. The distribution of clouds by size was controlled by the Kolmogorov statistical agreement criterion. The sample random cloud field generated with that procedure is shown in the Fig. 5. Cloud sizes are distributed according the Plank distribution (1) with  $D_m = 4$  km and  $\alpha = 1., \beta = 0.5, \eta = 1.0$ . Size of the whole cloud field area is  $100 \times 100$  km, relative sky coverage parameter  $S = 0.5$ .

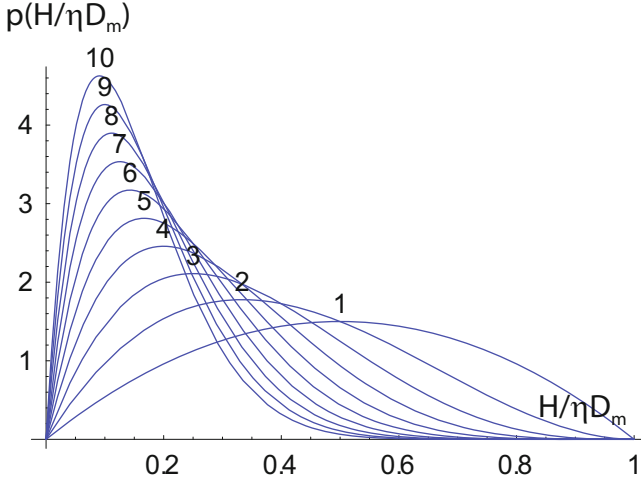


**Fig. 2.** Probability density functions of the cloud heights distribution (12) for different values of the distribution parameter  $p_0$  (indicated by numbers with corresponding curves).

### 3 Radiative Properties of the Clouds and the Atmosphere

The total absorption coefficient  $\gamma_\lambda(h)$  in a cloudy atmosphere consists of molecular absorption in oxygen and water vapor, as well as absorption in small cloud droplets. Absorption in molecular oxygen depends on temperature and pressure, information about it can be found, for example, in [7, 7, 23]. The absorption coefficient in water vapor, in addition, has a close to linear dependence on absolute humidity [21, 23, 24].

The size distribution of droplets of layered clouds and cumulus clouds of good weather is given in [25]. The average droplet sizes of these clouds are 3.9–7.5 microns, and the maximum contribution to the water content is made by droplets with a radius of 10–20 microns [19]. Radar studies by E. Gossard [26] show the presence of droplets with a radius of 70 microns or more in powerful cumulus clouds, and the largest contribution to water content is made by droplets with a size of about 50 microns.

Taking the scattering of microwave radiation on spherical water particles in a cloud by Rayleigh, it is not difficult to obtain the formula [2] for the volume absorption coefficient of the liquid droplet phase in the cloud [20]

$$k = \frac{3w}{\rho} k I m \left( \frac{m^2 - 1}{m^2 + 2} \right) \quad (17)$$

where  $w$  is the water content of the cloud,  $kg/m^3$ ,  $\rho$  is the density of water,  $kg/m^3$ ,  $k = \omega/c$  is the wave number of radiation,  $m$  is the refractive index of water.

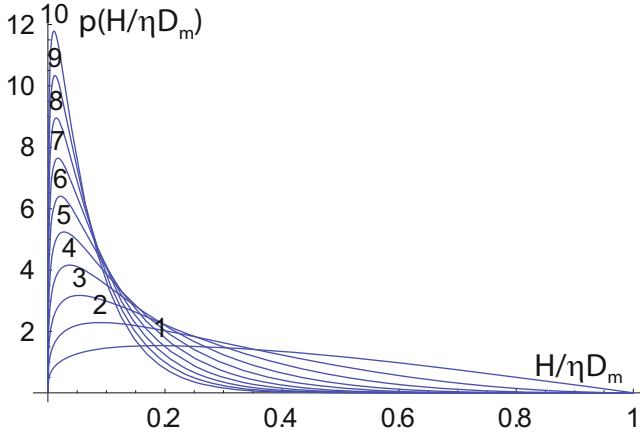


**Fig. 3.** Probability density functions of the cloud heights distribution (13) for different values of the distribution parameter  $p_0$  (indicated by numbers with corresponding curves).

The coefficients of absorption of radiation by water vapor and the values of total integral oxygen absorption in a vertical column of atmospheric air for different wavelengths can be calculated using the well-known formulas [23]. The complex permittivity of liquid water is determined by the Debye formula (see, for example, [2])

$$\varepsilon = \varepsilon_0 + \frac{\varepsilon_s - \varepsilon_0}{1 + i \frac{\Delta\lambda}{\lambda}} \quad (18)$$

where

$$\Delta\lambda = 2\pi\tau_p \frac{\varepsilon_s + 2}{\varepsilon_0 + 2} \quad (19)$$

$\varepsilon_s$  - static permittivity of water (at frequencies  $\nu \ll 1/\tau_p$ ),  $\varepsilon_0 = 4,9$  - optical permittivity of water (at frequencies  $\nu \gg 1/\tau_p$ ), relaxation time [3]

$$\tau_p = \exp\left[9,8 \left(\frac{273}{T + 273} - 0,955\right)\right] \cdot 10^{-12} s \quad (20)$$

The static permittivity of water is described by the approximate formula [3]

$$\varepsilon_s(T) = 88,045 - 0,4147 \cdot T + 6,295 \cdot 10^{-4} \cdot T^2 + 1,075 \cdot 10^{-5} \cdot T^3 \quad (21)$$

Values of temperature, water reserve and cloud power for Cu cong and Cu med are given in [2,30]. The altitude profile of the water content of each cloud was calculated using the formula [27,30]

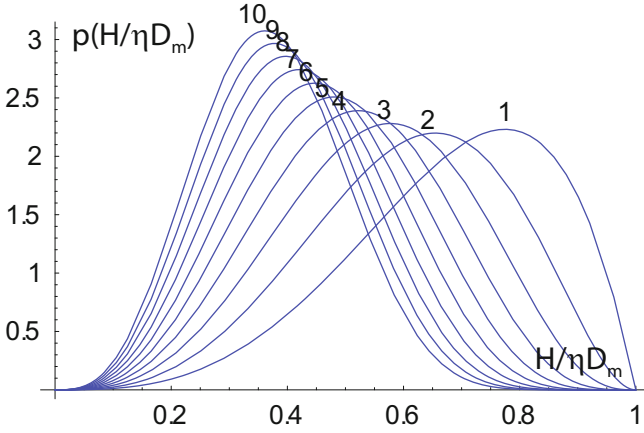


**Fig. 4.** Probability density functions of the cloud heights distribution (15) for different values of the distribution parameter  $p_0$  (indicated by numbers with corresponding curves).

$$w(\xi) = w(\xi_0) \frac{\xi^{\mu_0} (1 - \xi)^{\psi_0}}{\xi_0^{\mu_0} (1 - \xi_0)^{\psi_0}} = \frac{W}{H} \frac{\Gamma(2 + \mu_0 + \psi_0)}{\Gamma(1 + \mu_0) \Gamma(1 + \psi_0)} \xi^{\mu_0} (1 - \xi)^{\psi_0} \quad (22)$$

where  $\xi = h/H$  is the reduced height inside the cloud,  $H$  is the power of the cloud, km,  $W$  is the water reserve of the cloud,  $kg/m^2$ ,  $w(\xi_0)$  is the water content of the cloud,  $kg/m^3$ ,  $w$  is the maximum water content clouds,  $\xi_0$  – the reduced height of the maximum water content of the cloud,  $\mu_0, \psi_0$  - dimensionless parameters of the model. According to [30], the parameter values are  $\mu_0 = 3.27, \psi_0 = 0.67, \xi_0 = 0.83$ . The dependence of the water reserve of Cumulus-type clouds ( $kg/m^2$ ) on the cloud power (km) according to the tabular data given in [30] was approximated by the formula

$$W = 0,132574 \cdot H^{2,30215} \quad (23)$$

## 4 Microwave Thermal Radiation Simulation

In the microwave range, the influence of scattering processes in a cloudy atmosphere can be neglected. If the quantum energy at the radiation frequency is small compared to the temperature  $\hbar\omega \ll kT$ , the Planck function is almost proportional to the temperature, which is known as the so-called Rayleigh-Jeans approximation [4, 5]. Thus the observed intensity can be expressed directly in the radio brightness temperature  $T_b$  units (degrees). Under these conditions, and also under the assumption of local thermodynamic equilibrium, the radio brightness temperature of a plane-layered atmosphere when observed from the Earth's surface can be represented as [28, 29]



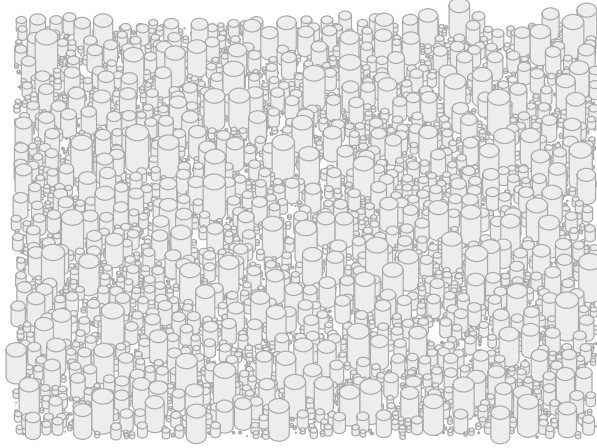


**Fig. 5.** Sample of the random cloud field model generated with the algorithm developed here. Cloud sizes are distributed according the Plank distribution (1) with  $D_m = 4$  km and  $\alpha = 1.$ ,  $\beta = 0.5$ ,  $\eta = 1.0$ . Size of the whole cloud field area is  $100 \times 100$  km, relative sky coverage parameter  $S = 0.5$ .

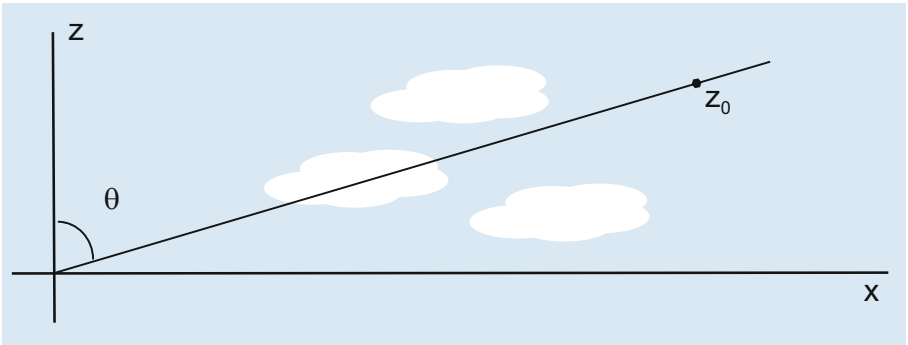


**Fig. 6.** Sounding ray direction.

$$T_b(\lambda, \theta) = \int_0^\infty T(z) \gamma_\lambda(z) \exp\left(-\int_0^z \gamma_\lambda(z') \sec\theta dz'\right) \sec\theta dz \quad (24)$$

where  $T(z)$  is the temperature of the atmosphere at an altitude of  $z$ ,  $\gamma_\lambda(z)$  is the total absorption coefficient,  $\theta$  is the zenith angle of the viewing direction (see the Fig. 6),  $\lambda$  is the wavelength. Similar integral equation can be written down also for the case of the space-borne observations

$$T_b(\lambda, \theta) = T_{b0} \exp\left(-\int_0^{z_0} \gamma_\lambda(z') \sec\theta dz'\right) + \quad (25)$$

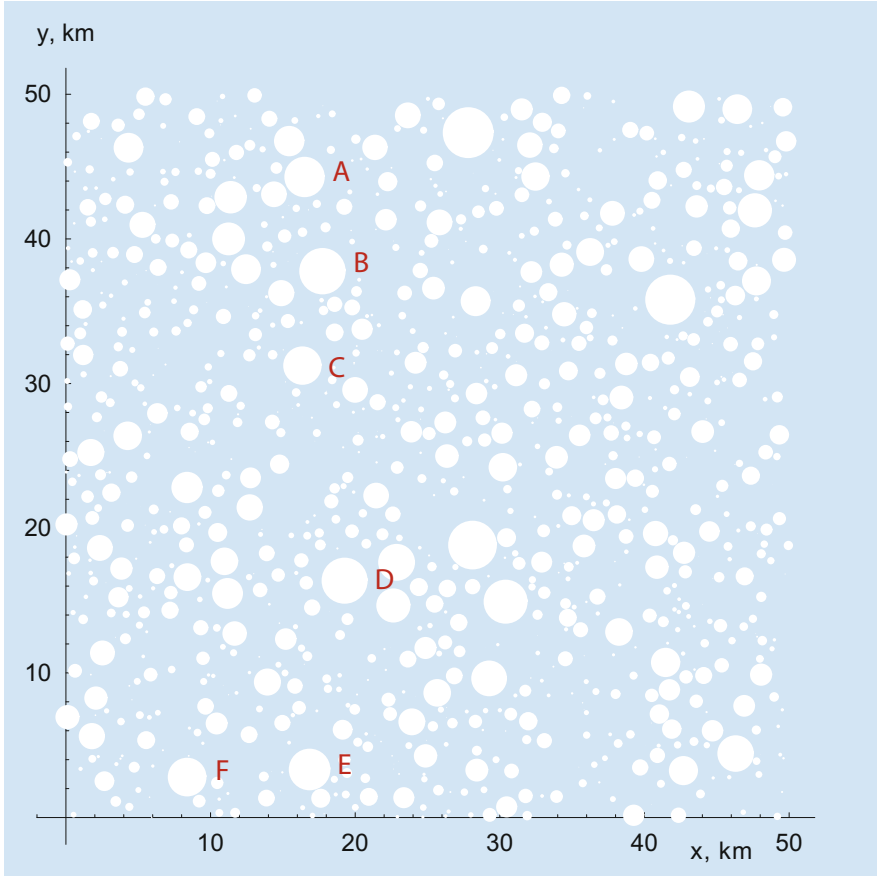


**Fig. 7.** 2D view of the cloud field portion used for the sample  $T_b$  simulation. Cloud sizes are distributed according the Plank distribution (1) with  $D_m = 4$  km and  $\alpha = 1.$ ,  $\beta = 0.5$ ,  $\eta = 1.0$ . Size of the whole cloud field area is  $50 \times 50$  km.

$$\int_0^{z_0} T(z) \gamma_\lambda(z) \exp\left(-\int_z^{z_0} \gamma_\lambda(z') \sec\theta dz'\right) \sec\theta dz,$$

where  $T_{b0}$  is the radio brightness temperature of the underlying surface.

The expressions (24) and (25) can be immediately integrated numerically, which readily yields the radio brightness temperature  $T_b$ . Repeating these calculations for a set of observation points and directions, one gets map of the radio brightness temperatures over the desired sea or land area.

## 5 Parallelization Efficiency Analysis

Since the integrand does not exhibit any singularities or irregularities, an integration procedure is rather simple. It can be easily parallelized dividing the integration domain or parametrically, using different threads for different sounding ray

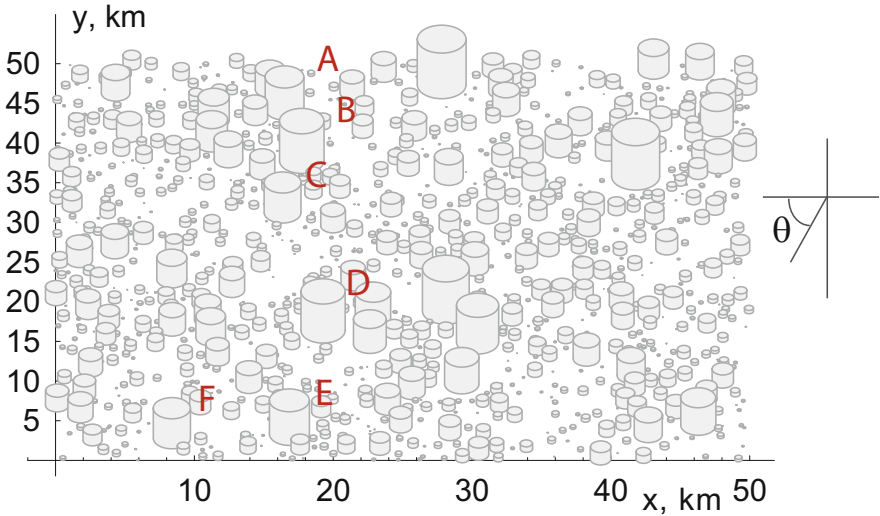


**Fig. 8.** 3D view of the cloud field portion used for the sample  $T_b$  simulation. Cloud sizes are distributed according to the Plank distribution (1) with  $D_m = 4$  km and  $\alpha = 1.$ ,  $\beta = 0.5$ ,  $\eta = 1.0$ . Size of the whole cloud field area is  $50 \times 50$  km.

trajectories. However, for realistic practical purposes these routine calculations should be performed for rather large areas covered by the clouds. In addition, to investigate statistical characteristics of the radio brightness distributions they should be repeated many times. This implies the ultimate need in using high-performance parallel computer systems. The algorithm itself can be implemented using only the basic parallel programming techniques, e.g. the OpenMP or MPI standards.

Since all the integrals (24) and (25) can be evaluated independently from each other, parallelization of these calculations is rather effective both on MPP and SMP architectures. Namely, the computing work can be distributed among any reasonable number of processing cores. Because the threads do not interact with each other, the acceleration is roughly proportional to the number of the cores used. For relatively small cloud fields, SMP architectures are rather effective in practice.

For example, we performed these calculations for the sample portion of the broken cloud field shown in the Figs. 7 and 8 over the sea surface ( $T_{b0} = 100$  K). The node with 8 computing cores (two 4-core CPUs) was used with the code using OpenMP standard. The result is shown in the Fig. 9. For simpler identification of characteristic features of the cloud field and corresponding features of the radio brightness map, we labeled some of them with the capital letters (A–F). Warm clouds can be clearly seen over the relatively cold sea surface. To account for the instrumental distortions, the calculated  $T_b$  map was convolved with the simple model Point Spreading Function (PSF). The PSF was chosen

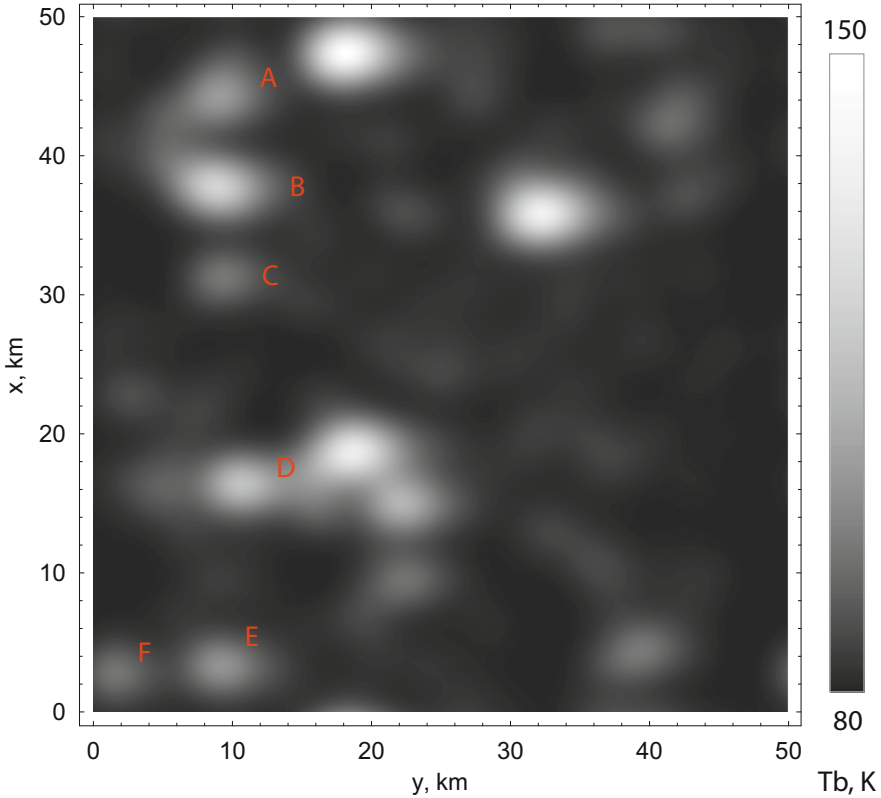


**Fig. 9.** Sample 2D mapping of the simulated distribution of the radio brightness temperature  $T_b$  (25) observed from space. Random cloud field is shown in the Figs. 7 and 8 over the sea surface ( $T_{b0} = 100\text{ K}$ ). Viewing zenith angle  $\theta = 70^\circ$ , radiometer frequency 70 GHz.

Gaussian with 2 km half width. This PSF is rather idealistic, however it is used here to show the distortion visually just for the illustrative purposes.

## 6 Conclusions and Remarks

In the course of the study, algorithms for generating cloud fields were developed based on well-known stochastic models of broken cumulus clouds proposed for real cloud distributions obtained empirically. For the obtained implementations of random cloud fields, numerical estimates of shading curves are made, i.e., the probability of sky overlap in a given direction, depending on the total cloud cover score. The estimates obtained are compared with published observational data on the probabilities of sky overlap.

As a result of the study, the compliance of the models of the broken cloud cover with the known observational data was verified. In addition, the developed

algorithms and computer models of cloud fields form a significant practical basis for further studies of radiation processes in the cloud atmosphere.

The research is carried out using the equipment of the shared research facilities of HPC computing resources at Lomonosov Moscow State University [31]. The authors thank both reviewers for valuable comments.

## References

1. Nicoll, G.R.: The measurement of thermal and similar radiations at millimetre wavelengths. *Proc. IEEE B Radio Electron. Eng.* **104**(17), 519–527 (1957)
2. Akvilonova, A.B., Kutuza, B.G.: Thermal radiation of clouds. *J. Com. Tech. Elect.* **23**(9), 1792–1806 (1978)
3. Ulaby, F.T., Moore, R.K., Fung, A.K.: *Microwave Remote Sensing, Active and Passive*, vol. 1. Addison-Wesley, Reading, MA (1981)
4. Drusch, M., Crewell, S.: Principles of radiative transfer. In: Anderson, M.G. (ed.) *Encyclopedia of Hydrological Sciences*. Wiley (2006)
5. Janssen, M.A. (ed.): *Wiley series in remote sensing and image processing*, Vol. 6, *Atmospheric Remote Sensing by Microwave Radiometry*, 1st edn. Wiley (1993)
6. Schloerb, P.F., Keihm, S., Von Allmen, P., et al.: *Astron. Astrophys.* **583** (2015)
7. Zhevakin, S.A., Naumov, A.P.: *Radio Eng. Electron.* **19**, 6 (1965)
8. Zhevakin, S.A., Naumov, A.P.: *Izv. Univ. Radiophys.* **10**, 9–10 (1967)
9. Staelin, D.H., et al.: Microwave spectrometer on the Nimbus 5 satellite meteorological and geophysical data. *Science* **182**(4119), 1339–1341 (1973)
10. Ilyushin, Y.A., Hartogh, P.: Submillimeter wave instrument radiometry of the Jovian icy moons-numerical simulation of the microwave thermal radiative transfer and Bayesian retrieval of the physical properties. *Astron. Astrophys.* **644**, A24 (2020)
11. Hagfors, T., Dahlstrom, I., Gold, T., Hamran, S.-E., Hansen, R.: *Icarus* **130** (1997)
12. Kutuza, B.G., Smirnov, M.T.: The influence of clouds on the averaged thermal radiation of the Atmosphere-Ocean surface system. *Earth Studies from Space* (No. 3) (1980)
13. Egorov, D.P., Ilyushin, Y.A., Koptsov, Y.V., Kutuza, B.G.: Simulation of microwave spatial field of atmospheric brightness temperature under discontinuous cumulus cloudiness. *J. Phys: Conf. Ser.* **1991**(1), 012015 (2021)
14. Egorov, D.P., Ilyushin, Y.A., Kutuza, B.G.: Microwave radiometric sensing of cumulus cloudiness from space. *Radiophys. Quantum Electron.* **64**, 564–572 (2022). <https://doi.org/10.1007/s11141-022-10159-2>
15. Ilyushin, Y.A., Kutuza, B.G., Sprenger, A.A., Merzlikin, V.G.: Intensity and polarization of thermal radiation of three-dimensional rain cells in the microwave band. *AIP Conf. Proc.* **1810**(1), 040003 (2017)
16. Ilyushin, Y., Kutuza, B.: Microwave radiometry of atmospheric precipitation: radiative transfer simulations with parallel supercomputers. In: Voevodin, V., Sobolev, S. (eds.) *RuSCDays 2018. CCIS*, vol. 965, pp. 254–265. Springer, Cham (2019). [https://doi.org/10.1007/978-3-030-05807-4\\_22](https://doi.org/10.1007/978-3-030-05807-4_22)
17. Ilyushin, Y.A., Kutuza, B.G.: Microwave band radiative transfer in the rain medium: implications for radar sounding and radiometry. In: *2017 Progress in Electromagnetics Research Symposium-Spring (PIERS)*, pp. 1430–1437. IEEE (2017)

18. Ilyushin, Y.A., Kutuza, B.G.: New possibilities of the use of synthetic aperture millimeter-wave radiometric interferometer for precipitation remote sensing from space. In: 2013 International Kharkov Symposium on Physics and Engineering of Microwaves, Millimeter and Submillimeter Waves, pp. 300–302. IEEE (2013)
19. Mazin, I.P., Shmeter, S.M. (eds.): Cumulus clouds and associated deformation of meteorological element fields. In: Proceedings of the CAO. Hydrometeoizdat, Moscow Issue 134 (1977)
20. Ilyushin, Y.A., Kutuza, B.G.: Influence of a spatial structure of precipitates on polarization characteristics of the outgoing microwave radiation of the atmosphere. *Izv. Atmos. Ocean. Phys.* **52**(1), 74–81 (2016). <https://doi.org/10.1134/S0001433816010047>
21. Barrett, A.H., Chung, V.K.: *J. Geophys. Res.* **67** (1962)
22. Plank, V.G.: The size distribution of cumulus clouds in representative Florida populations. *J. Appl. Meteorol. Climatol.* **8**(1), 46–67 (1969)
23. Rec. ITU-R P.676-3 1 recommendation ITU-R P.676-3 attenuation by atmospheric gases (Question ITU-R 201/3) (1990-1992-1995-1997)
24. Zhevakin, S.A., Naumov, A.P.: *Izv. Univ. Radiophys.* **6**, 4 (1963)
25. Hrgian, A.H.: *Atmospheric Physics*. Hydrometeoizdat (1969)
26. Gossard, E.E.: The use of radar for studies of clouds. *Proc. Wave Prop. Lab, NOAA/ERL* (1978)
27. Voit, F.Y., Mazin, I.P.: Water content of cumulus clouds. *Izv. Akad. Nauk SSSR, Fiz. Atmos. Okeana* **8**(11), 1166–1176 (1972)
28. Kislyakov, A.G., Stankevich, K.S.: Investigation of tropospheric absorption of radio waves by radio astronomy methods. *Izv. VUZov, Radiophys.* **10**(9–10) (1967)
29. Kondratyev, K.Y.: Radiant heat transfer in the atmosphere. Hydrometeoizdat (1956)
30. Kutuza, B.G., Danilychev, M.V., Yakovlev, O.I.: Satellite monitoring of the earth: microwave radiometry of the atmosphere and surface (2017)
31. Sadovnichy, V., Tikhonravov, A., Voevodin, V., Opanasenko, V.: “Lomonosov”: supercomputing at Moscow state university. In: *Contemporary High Performance Computing: From Petascale Toward Exascale*. Chapman & Hall/CRC Computational Science, Boca Raton (2013)